Exploring Applicable Scenarios and Boundary of MAC Protocols: A MAC Performance Analysis Framework for Underwater Acoustic Networks

Jiani Guo, Shanshan Song, *Member, IEEE*, Jun Liu, *Member, IEEE*, Hao Chen, Yuanbo Xu, and Jun-Hong Cui, *Member, IEEE*

***Abstract*—Medium Access Control (MAC) protocols are critical for scheduling resources to access multiple users without collisions in Underwater Acoustic Networks (UANs). Due to harsh marine environments and limited communication resources, UANs lack a standard MAC protocol to adapt to various scenarios. The specific UAN scenario suffers from how to analyze multiple basic MAC protocols' performance boundaries and modify the most potential one. A practical solution is to evaluate MAC protocols' performance by modeling data loss (collisions and packet errors) and service time. However, existing models provide inaccurate performance results, since they ignore the effects of unique UANs' characteristics and MAC protocol diversity on data loss and service time. In this paper, we propose a MAC Performance Analysis Framework (MPAF) for UANs to consider both unique UANs' characteristics and MAC protocols' diversity. We design Successful Transmission Probability (STP) model and Packet Service Time (PST) model in MPAF to estimate nodal throughput, delay, and energy consumption. STP model analyzes data loss types of different MAC protocols by considering long propagation delay, half-duplex communication, and random backoff to achieve a superior STP result from a view of real underwater communication conditions. Based on STP model, we employ Markov chain to deduce the retransmission number in PST model. In this way, MPAF ensures effectiveness and applicability in real-ocean environments. Extensive simulation results show that MPAF can accurately evaluate different MAC protocols' performance boundaries, select the most appropriate basic protocol, and provide modified suggestions for a specific UAN scenario.**

***Index Terms*—Underwater acoustic network, performance analysis framework, Medium Access Control (MAC) protocols.**

Manuscript received 14 September 2023; revised 20 May 2024; accepted 18 June 2024. Date of publication 24 June 2024; date of current version 5 November 2024. This work was supported in part by National Key Research and Development Program of China under Grant 2021YFC2803000 and in part by the National Natural Science Foundation of China under Grant 62101211. Recommended for acceptance by J. Choi. *(Corresponding author: Shanshan Song.)*

Jiani Guo, Shanshan Song, Hao Chen, and Yuanbo Xu are with the College of Computer Science and Technology, Jilin University, Changchun 130012, China (e-mail: jnguo20@mails.jlu.edu.cn; songss@jlu.edu.cn; chenhao2118@mails.jlu.edu.cn; yuanbox@jlu.edu.cn).

Jun Liu is with the School of Electronic and Information Engineering, Beihang University, Beijing 100191, China, and also with the Smart Ocean Technology Co., Ltd, Shenzhen 518055, China (e-mail: liujun2019@buaa.edu.cn).

Jun-Hong Cui is with the College of Computer Science and Technology, Jilin University, Changchun 130012, China, and also with the Shenzhen Ocean Information Technology Industry Research Institute, Shenzhen 518055, China (e-mail: junhong_cui@jlu.edu.cn).

Digital Object Identifier 10.1109/TMC.2024.3417895

I. Introduction

UNDERWATER Acoustic Network (UAN) has become an attractive spot for underwater research. It equips various sensors and vehicles to achieve marine applications, such as underwater data collection [1], environmental observation [2], and mining exploration [3]. In UANs, Medium Access Control (MAC) protocols are crucial because they determine nodes' access and resource allocation rules. Due to harsh marine environments and limited communication resources, underwater MAC protocols lack universality for various scenarios. For a specific UAN, it expects to match an appropriate MAC protocol from multiple candidates to achieve the task with high performance and low costs. Therefore, performance analysis is an indispensable process to select the optimal basic MAC protocol and provide modified suggestions for a UAN before real sea trials.

To explore underwater MAC protocols' performance, researchers have proposed some analysis models. The earlier model studies a single MAC protocol and still adopts analysis methods of terrestrial networks [4]. Gradually, partial UANs' characteristics, such as long preamble and low transmission rate, are considered in MAC protocols' analysis models [5]. As the research moves along, effects of MAC protocols' diversity on performance are studied in some models [6]. We summarize existing works and find that data loss (collisions and packet errors) and service time are two significant factors that influence underwater MAC protocols' performance.

However, unique UANs' characteristics pose great challenges to analyze data loss and service time. 1) *Various data loss:* Most underwater acoustic modems employ half-duplex communication that does not allow a node to send and receive simultaneously, leading to more collision types in UANs than in terrestrial networks. Moreover, these collision types are strongly related to detailed operations of the specific MAC protocol. 2) *Irregular service time:* The underwater propagation speed is about 1500 m/s, which is five orders of magnitude smaller than that in terrestrial networks. Non-negligible long propagation delay further aggravates data loss and retransmission, making modems always in a non-idle state. As a result, the packet processing in MAC protocols no longer obeys the well-defined parametric distribution, such as Poisson distribution, but strongly depends on the specific MAC protocol operation. Most existing

underwater analysis models lack systematical consideration of the above challenges while simplifying the modeling of significant protocols' details. They are difficult to summarize overall data loss types and quantify the probability of each type. Finally, they calculate inaccurate successful transmission probability and service time, failing to analyze real-ocean communication scenarios.

In this paper, we design a MAC Performance Analysis Framework (MPAF) for UANs by considering both UANs' characteristics and MAC protocols' diversity. MPAF analyzes three performance metrics: nodal throughput, delay, and energy consumption via two models: Successful Transmission Probability (STP) model and Packet Service Time (PST) model. In STP model, we derive data loss types for various MAC protocols by considering half-duplex communication, random backoff, and long propagation delay to achieve a superior STP result. Combined with this STP model, we deduce the retransmission number based on Markov chain to make PST model consistent with real-ocean communication scenarios.

We highlight the main contributions as follows:

- Propose a framework that considers both unique UANs' characteristics and protocols' diversity to simultaneously evaluate underwater MAC performance, including nodal throughput, delay, and energy consumption.
- Model STP and PST in the proposed MPAF. STP model analyzes comprehensive data loss types to improve the effectiveness and applicability of MPAF in real-ocean communication scenarios. Based on the STP model, PST model considers retransmissions to evaluate the service delay of different MAC protocols for packets.
- Design experiments to evaluate the effectiveness of MPAF, and analyze the impacts of channel quality, input traffic, and node density on different MAC protocols. Extensive experiments demonstrate that MPAF is more consistent with real-ocean communication scenarios than the state-of-the-art models in [5], [6], [7], [8]. The results also show that MPAF can provide the most appropriate basic protocol and modified suggestions for various scenarios.

The rest of this paper is organized as follows: We briefly discussed related works in Section II. Preliminaries are described in Section III. In Section IV, MPAF framework is discussed in detail from STP model, PST model, and performance metrics. Subsequently, we analyze simulation results in Section V. Finally, the conclusion and future work are provided in Section VI.

II. Related Work

In this section, we briefly introduce underwater MAC protocols and their previous performance analysis models.

A. Medium Access Control Protocols

MAC protocols for UANs are divided into two categories: non-competitive protocols and competitive protocols [9]. Non-competitive protocols include Time/Frequency/Code Division Multiple Access (TDMA/FDMA/CDMA)-based protocols. Considering low bandwidth and changeable channels, UANs prefer TDMA-based protocols, because they are independent of bandwidth and channel quality. These protocols allocate an individual sending slot to each node. By separating the sending time, TDMA-based protocols avoid data collisions [10], [11], [12]. As for competitive protocols, random-access-based protocols and handshake-based protocols are two classic protocols [13]. Random-access-based protocols randomly send packets without considering collisions [14]. Handshake-based protocols make some transmission negotiations to decrease data collisions.

B. Performance Analysis Models of MAC Protocols

In actual UANs, most MAC protocols are improvements or combinations of TDMA-based protocols, random-access-based protocols, and handshake-based protocols (we call these three protocols as basic protocols in later sections). These improved protocols' analysis are simpler since they eliminate some data loss in basic protocols. Therefore, most existing models consider the above three MAC protocols to analyze performance. In [4] modified slots' length for slotted ALOHA, and designed a theoretical model to analyze throughput. In [5] proposed nodal throughput and collision probability models for ALOHA and Slotted Floor Acquisition Multiple Access (S-FAMA) by considering low transmission rate and long preambles. In [6] conducted packet queuing delay and packet error probability based on a random-access-based protocol and a handshake-based MAC protocol. In [7] employed the characteristic of underwater half-duplex communication to develop a successful transmission probability model for ALOHA. In [15] modeled throughput and communication overhead to compare the performance of different MAC protocols. In addition, [16] considered different typologies and data rates to compare the performance of slotted ALOHA and an RTC/CTS-based MAC protocol.

The above models fail to consider comprehensive UANs' characteristics in analyzing data loss types, and neglect effects of long propagation delay on packet processing pattern. Therefore, these models evaluate inaccurate MAC protocols' performance in real-ocean scenarios.

III. Preliminaries

In this section, we introduce performance metrics. Then we formulate a MAC protocols' performance analysis problem, and design a framework to solve it.

A. Evaluation Metrics

We select nodal throughput, delay, and energy consumption as evaluation metrics, due to their comprehensiveness, availability, and weak correlation [17].

Nodal throughput as the rate of completions at a node is denoted as follows:

$$T_h = \frac{L_b P_s}{T_s}, \tag{1}$$

where L_b is the size of data bits, P_s is the successful transmission probability, and T_s is the MAC protocol's total service time for L_b bits.

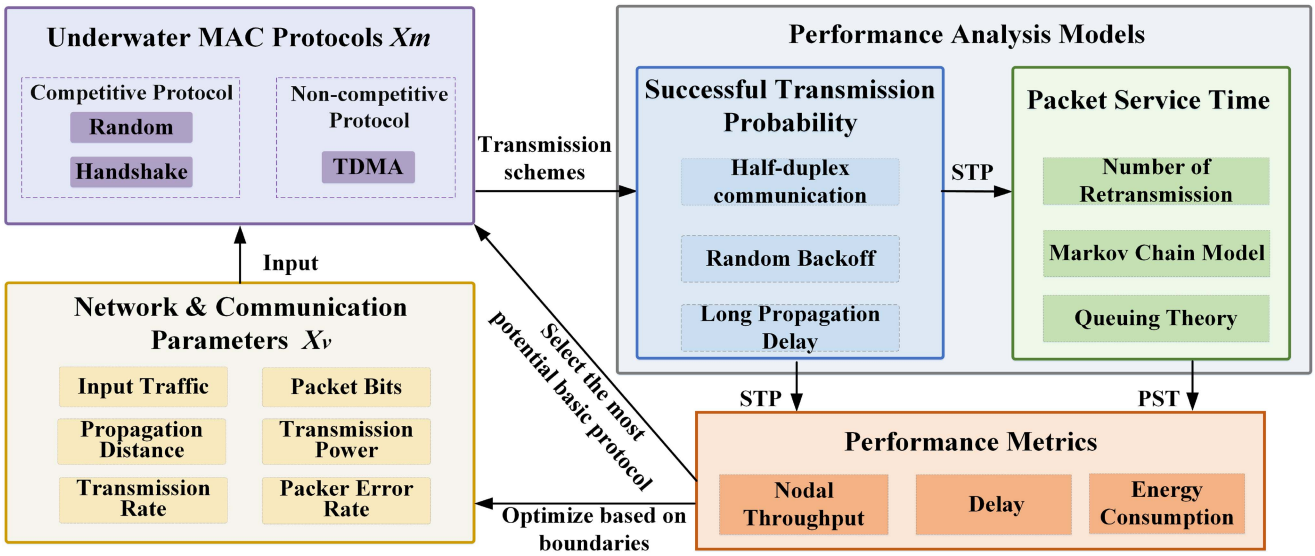

Fig. 1. The architecture of MPAF. Input network and communication parameters X_v into different MAC protocols X_m. Then MPAF designs STP model and PST model to calculate performance metrics. Based on these metrics' results, MPAF selects the optimal protocol and parameters for a specific UAN scenario.

We define delay as S_t, including the whole transmission, propagation, and queuing delay based on retransmission.

Energy consumption of a packet is calculated as follows:

$$E = P_{sp} T_r, \tag{2}$$

where P_{sp} is the transmission power, and T_r is the total transmission time considering retransmission.

It is worth noting that L_b and P_{sp} are known input variables. S_t and T_r are calculated by T_s based on queuing theory. Only Successful Transmission Probability (STP) P_s and Packet Service Time (PST) T_s are unknown. Therefore, they are two key factors to calculate the three metrics.

B. Problem Formulation

Based on above analysis, we build STP model and PST model to analyze different MAC protocols' performance, then select the optimal protocol and parameters. Let X_v denote a set of known network and communication variables, including input traffic λ, packet bits L_b, transmission power P_{sp}, propagation distance d, packet error rate P_e, and transmission rate TR, $X_v = \{\lambda, L_b, P_{sp}, d, P_e, TR\}$. We define $X_m = \{xm_1, xm_2 \ldots xm_o, N\}$ as a set of o MAC protocols with the maximum retransmission number N in the MAC layer.

Given network and communication variables set X_v and MAC protocols set X_m as inputs, STP model outputs the successful transmission probability of a single transmission:

$$P_s = \mathrm{STP}(X_v, X_m). \tag{3}$$

P_s is the precondition of T_s. Based on P_s, PST model derives the expected transmission times and calculates packet service time for different MAC protocols:

$$T_s = \mathrm{PST}(P_s, X_m). \tag{4}$$

We calculate performance metrics in Section III-A with P_s and T_s, and output a basic MAC protocol which provides the optimal throughput, delay, or energy consumption based on a specific UAN scenario requirements:

$$xm_o^* = \arg\max_{xm_o} \left\{ T_h | \frac{1}{S_t} | \frac{1}{E} \right\}. \tag{5}$$

With the specific xm_o^* MAC protocol, we optimize network and communication variables to further explore performance boundaries:

$$X_v{}^* = \arg\max_{X_v} \left\{ T_h(xm_o^*) | \frac{1}{S_t(xm_o^*)} | \frac{1}{E(xm_o^*)} \right\}. \tag{6}$$

C. Design Architecture

To address the above problem, we design a MAC Performance Analysis Framework (MPAF) to analyze performance metrics by considering both MAC protocols' diversity and unique UANs' characteristics, as represented in Fig. 1.

We first input given network and communication parameters X_v into different MAC protocols X_m: a TDMA-based protocol, ALOHA (random-access-based) protocol, and S-FAMA (handshake-based) protocol [9]. Based on these protocols, we design STP model and PST model to calculate P_s and T_s. Specifically, STP model analyzes data loss types of each protocol with the consideration of half-duplex communication, random backoff, and long propagation delay. With the STP result, PST model derives retransmission number via Markov chain, then calculates T_s via queuing theory.

The proposed MPAF calculates evaluation metrics via above two models. To improve the specific UAN's performance, we select the optimal MAC protocol. Based on metrics' boundaries results, we further optimize network and communication parameters.

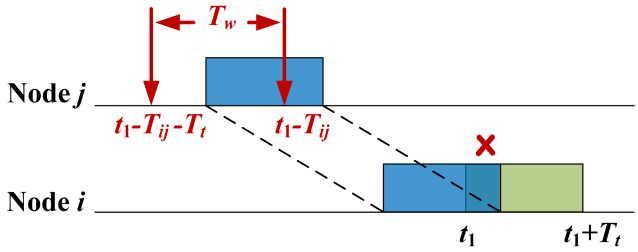

Fig. 2. Collisions at the sender caused by neighbors and itself. To avoid affecting node i's sending, neighbor node j should not send packets during $[t_1 - T_{ij} - T_t, t_1 - T_{ij}]$.

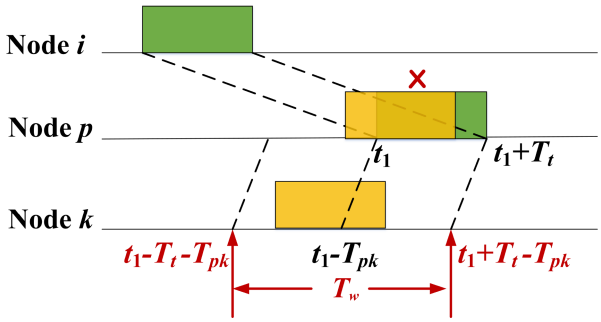

Fig. 3. Collisions at the receiver caused by hidden terminals. Node i is a sender, node p is a receiver, and node k is a hidden terminal. To avoid affecting node p's reception, node k should not send packets during $[t_1 - T_t - T_{pk}, t_1 + T_t - T_{pk}]$.

IV. MAC Performance Analysis Framework

In this section, we discuss the proposed MPAF in detail. Then we calculate performance metrics based on MPAF, including nodal throughput, delay, and energy consumption.

A. Successful Transmission Probability for Different MAC Protocols

1) Modeling of TDMA: In Time Division Multiple Access (TDMA) protocols, nodes transmit packets with different slots [10]. We set the total number of slots to m, and each node only sends one data packet at the beginning of its own slot. When a node has a packet in its sending queue, we denote the successful transmission probability as follows:

$$\dot{P}_s = \frac{1 - P_e(L_b)}{m}, \tag{7}$$

which means the node sends a data packet in its own slot without errors.

In addition, the sender needs to receive an acknowledgment (ACK) packet from the receiver in the same slot. Otherwise, the sender will re-transmit the data packet. We assume the ACK packet bits as L_b^a, and its successful transmission probability is calculated as follows:

$$\dot{P}_a = (1 - P_e(L_b^a)). \tag{8}$$

2) Modeling of ALOHA: In ALOHA protocol, nodes randomly send data packets [18]. In this way, besides packet errors, collisions also result in data loss. We discuss all collision types caused by UANs' characteristics to deduce STP. It is worth noting that collisions are generated between one-hop neighbors, and we assume such signal interference is strong. Once collisions occur, data packets are discarded.

Sender Collisions (SC): Take Fig. 2 as an example, node i expects to send a packet at time t_1. T_{ij} is the propagation delay of node i and node j, and T_t is the transmission delay of a data packet. Node j is a neighbor of node i. If node j or node i itself sends a packet during $[t_1 - T_{ij} - T_t, t_1 - T_{ij}]$, node i fails to send a packet at preset time t_1.

We set $\widetilde{P}_{sc}$ to indicate the probability that SC does not occur. Due to half-duplex communication in UANs, nodes disallow a new communication to abort the current communication. If node i's neighbors and itself are busy sending or receiving during collision window $\widetilde{T}_w$, they do not generate new communication to cause SC. Here we denote $\widetilde{\rho}$ as the probability that a node wants to send a packet based on M/G/1, and it is calculated as follows:

$$\widetilde{\rho} = \lambda \widetilde{T}_s, \tag{9}$$

where λ is the input traffic and $\widetilde{T}_s$ is the packet service time. In this case, $\widetilde{T}_w = T_t$, the sending length of a node during $\widetilde{T}_w$ is derived as follows:

$$\widetilde{T}_{ws} = \widetilde{\rho} \frac{T_t}{W_a + b_o} \widetilde{T}_w, \tag{10}$$

where W_a is the time for waiting an ACK packet, and b_o is the random backoff period. Due to long W_a, the number of sent packets $\frac{T_{ws}}{T_t} \ll 1$, and we can use it to represent sending probability of a node during $\widetilde{T}_w$ approximately. Therefore, $\widetilde{P}_{sc}$ can be derived as follows:

$$\widetilde{P}_{sc} = \left(1 - \frac{T_{ws}}{T_t}\right)^{\widetilde{n}+1}, \tag{11}$$

where $\widetilde{n}$ is the neighbors' number of node i.

Hidden Terminals Collisions (HTC): Node k is a neighbor of node p, but is out of node i's communication range. When node i communicates with node p, node k is a hidden terminal of node i.

If node k sends a packet during $\widetilde{T}_w$ period shown in Fig. 3, node p fails to receive a packet from node i. We define $\widetilde{P}_{hc}$ as the probability that all hidden terminals do not send packets during $\widetilde{T}_w$ due to busy terminal. The size of $\widetilde{T}_w$ is $2T_t$, and we put it into (10) then $\widetilde{P}_{hc}$ is calculated as follows:

$$\widetilde{P}_{hc} = \left(1 - \frac{2\widetilde{\rho} T_t}{W_a + bo}\right)^{\widetilde{n}_h}, \tag{12}$$

where $\widetilde{n}_h$ is the hidden terminals' number of node i.

Common Neighbors Collisions (CNC): node q is a common neighbor of node i and node p. When node i sends a packet to node p, node q can not interfere node i's sending or node p's reception. The influence of node q to node i has been discussed in **SC**. Therefore, here we only analyze how node q affects node p's reception.

As represented in Fig. 4, three nodes form only a triangle or a line. Based on the triangle theorem, we obtain distance

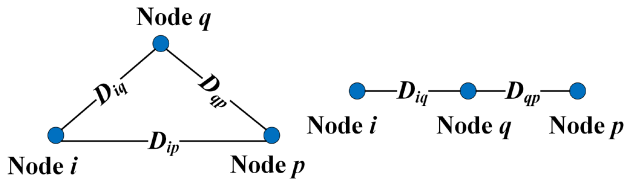

Fig. 4. Location relationship of any three nodes. D denotes the distance between two nodes.

relationship as follows:

$$\begin{cases} D_{ip} - D_{qp} \le D_{iq}; \\ D_{qp} - D_{iq} \le D_{ip}. \end{cases} \tag{13}$$

According to the relationship between distance and time, we transfer distance information in (13) into time information. Then we obtain T_w range as $[\max\{t_1 - T_{iq}, t_1 + T_{ip} - T_{qp} - T_t\}, \min\{t_1 + T_{iq}, t_1 + T_{ip} - T_{qp} + T_t\}]$, which means that **CNC** only has four types.

Fig. 5 shows these four collisions in detail. Take Fig. 5(a) as an example, node q does not send a packet during $[t_1 - T_{iq} - T_t, t_1 - T_{iq}]$ due to **SC**. In addition, if node q sends a packet during $[t_1 - T_{iq}, t_1 + T_{iq}]$, it will interfere node p's reception. Therefore, the value of $\widetilde{T}_{w\_1}$ is $2T_{iq}$. Similarly, we can obtain collision window values of other conditions: $\widetilde{T}_{w\_2} = T_t + T_{ip} - T_{qp} + T_{iq}$, $\widetilde{T}_{w\_3} = 2T_t$, and $\widetilde{T}_{w\_4} = T_{iq} - T_{ip} + T_{qp} + T_t$.

In these conditions, probability that a common neighbor does not send packets during collision window due to busy terminal is calculated as follows:

$$\widetilde{P}_{cc\_\widetilde{i}} = \left(1 - \frac{\widetilde{\rho}\widetilde{T}_{w\_\widetilde{i}}}{W_a + bo}\right)^{\widetilde{n}_{c\_\widetilde{i}}}, \tag{14}$$

where $\widetilde{i} = 1, 2, 3, 4$, and $\widetilde{n}_{c\_\widetilde{i}}$ is the number of common neighbors in condition $\widetilde{i}$. We finally get total $\widetilde{P}_{cc}$ as follows:

$$\widetilde{P}_{cc} = \prod_{\widetilde{i}=1}^{4} \widetilde{P}_{cc\_\widetilde{i}}. \tag{15}$$

Receiver Collisions (RC): node p is a receiver of node i, and is also a common neighbor of itself and node i. As described above, if node p sends a packet during $\widetilde{T}_w$, it will affect itself to receive a packet from node i.

As represented in Fig. 6, node p does not send a packet during $[t_1 - T_{ip} - T_t, t_1 - T_{ip}]$ and $[t_1 + T_{ip} - T_t, t_1 + T_{ip}]$, to avoid **SC** and **CNC**. There are two collisions conditions at the receiver: $t_1 - T_{ip} < t_1 + T_{ip} - T_t$, and $t_1 - T_{ip} > t_1 + T_{ip} - T_t$. Therefore, collision window $\widetilde{T}_w$ is calculated as follows:

$$\widetilde{T}_w = \begin{cases} T_t, & T_{ip} \ge 0.5T_t; \\ 2T_{ip}, & 0 < T_{ip} < 0.5T_t. \end{cases} \tag{16}$$

If node p does not send a packet during $\widetilde{T}_w$, then the network avoids **RC** collisions. This probability $\widetilde{P}_{rc}$ is denoted as follows:

$$\widetilde{P}_{rc} = 1 - \frac{\widetilde{\rho}\widetilde{T}_w}{W_a + b_o}. \tag{17}$$

Random Backoff Collisions (RBC): The sender sends a packet at time t_1, and a hidden terminal or a common neighbor sends a packet after Δt. If there is a collision between these two packets, the sender will retransmit the packet at time $T_A = t_1 + W_a + b_{o1}$, while the other node will retransmit its packet at time $T_B = t_1 + \Delta t + W_a + b_{o2}$. Specially, b_{o1} and b_{o2} are random backoff periods following $b_o \sim U(T_t, \beta T_t)$, and $\beta \ge 2$ is a constant. If $|T_B - T_A| < T_t$, a conflict occurs again at the receiver.

We calculate that $|T_B - T_A| = |\Delta t + b_{o2} - b_{o1}|$, where $\Delta t \sim U(0, T_t)$. First, we set $h = \Delta t + b_{o2}$, the Probability Distribution Function (PDF) of h can be derived as follows with convolution calculation:

$$f_h(h) = \begin{cases} \frac{h - T_t}{(\beta-1){T_t}^2}, & T_t < h < 2T_t; \\ \frac{1}{(\beta-1)T_t}, & 2T_t \le h \le \beta T_t; \\ \frac{1}{(\beta-1)T_t} - \frac{h - \beta T_t}{(\beta-1){T_t}^2}, & \beta T_t < h < (\beta+1)T_t; \\ 0, \quad \text{else.} \end{cases} \tag{18}$$

Second, we set $l = h - b_{o1}$, and the PDF of l is calculated as follows:

$$f_l(l) = \begin{cases} \frac{2l + 2\beta T_t - 3T_t}{2(\beta-1)^2{T_t}^2}, & (1-\beta)T_t < l < 0; \\ \frac{-2\,l^2 + 2T_t l + (2\beta - 3){T_t}^2}{2(\beta-1)^2{T_t}^3}, & 0 \le l \le T_t; \\ \frac{\beta}{(\beta-1)T_t} - \frac{l + T_t}{(\beta-1){T_t}^2} + \frac{1}{2(\beta-1)^2 T_t}, & T_t < l \le (\beta-1)T_t; \\ \frac{1}{(\beta-1)T_t}\left(\frac{\beta+1}{\beta-1} - \frac{1}{2(\beta-1)} - \frac{l+T_t}{(\beta-1)T_t}\right. & \\ \left. + \frac{(l + T_t - \beta T_t)^2}{2(\beta-1){T_t}^2}\right), & (\beta-1)T_t < T_t \le \beta T_t; \\ 0, \text{ else.} \end{cases} \tag{19}$$

Finally, we can obtain the probability that **RBC** does not occur as follows:

$$\widetilde{P}_{dc} = 1 - \int_{-T_t}^{T_t} f_l(l)dl. \tag{20}$$

Based on above collisions analysis, the STP of a data packet for its first transmission is calculated as follows:

$$\widetilde{P}_s(1) = (1 - P_e)\widetilde{P}_{sc}\widetilde{P}_{hc}\widetilde{P}_{cc}\widetilde{P}_{rc}. \tag{21}$$

STP considers **RBC** from the second transmission. **HTC** or **CNC** are preconditions of **RBC**. Considering all hidden terminals $\widetilde{n}_h$ and common neighbors $\widetilde{n}_c$, the sum probability that neither **RBC**'s preconditions nor itself occurs is calculated as follows:

$$\widetilde{P}_{bc} = \sum_{\gamma=1}^{\widetilde{n}_h + \widetilde{n}_c} \frac{C_{\widetilde{n}_h + \widetilde{n}_c}^{\gamma}}{\sum_{\epsilon=1}^{\widetilde{n}_h + \widetilde{n}_c} C_{\widetilde{n}_h + \widetilde{n}_c}^{\epsilon}} (1 - \widetilde{P}_{dc})^{\gamma} \left(\sqrt{\widetilde{P}_{hc}\widetilde{P}_{cc}}\right)^{\widetilde{n}_h + \widetilde{n}_c - \gamma}. \tag{22}$$

We assume the maximum number of transmissions is N, and the STP of nth $(2 \le n \le N)$ transmission considers whether random backoff occurs in the $n-1$th transmission. We define the probability that nth transmission occurs random backoff as

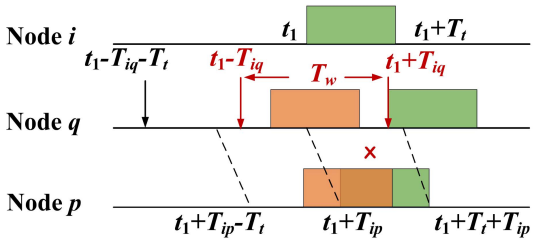

(a) The first collision type

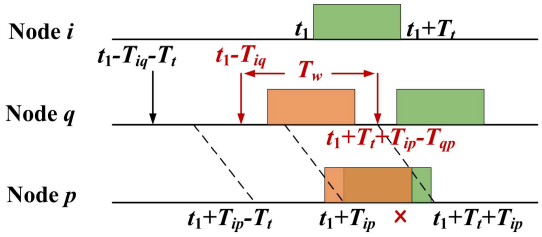

(b) The second collision type

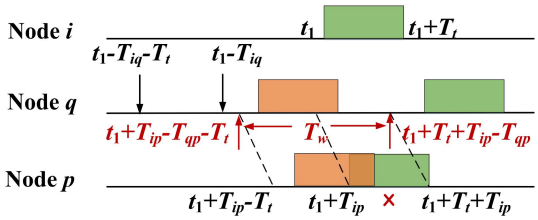

(c) The third collision type

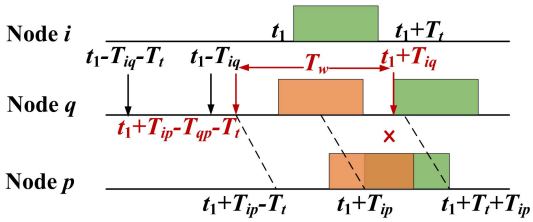

(d) The fourth collision type

Fig. 5. Collisions at the receiver caused by common neighbors. Node i is a sender, node p is a receiver, and node q is common neighbor of node p and node i. Node q in this scenario can not affect either node i's sending or node p's reception.

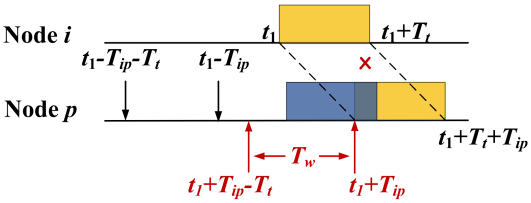

(a) The first collision type

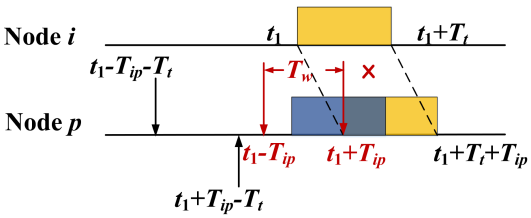

(b) The second collision type

Fig. 6. Collisions at the receiver caused by itself. Node i is a sender, and node p is a receiver. Node p should not send a packet during T_w to avoid affecting its own reception.

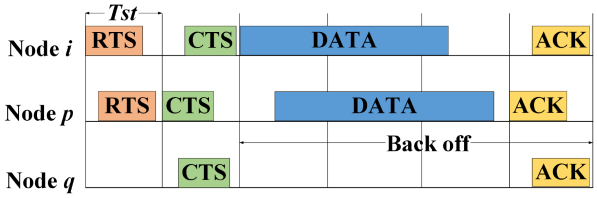

Fig. 7. Transmission process of S-FAMA.

follows:

$$\widetilde{P}_{rb}(n)=\begin{cases}\widetilde{P}_{sc}(1-\widetilde{P}_{hc}\widetilde{P}_{cc}), & n=1;\\ \widetilde{P}_{rb}(n-1)\widetilde{P}_{sc}(1-\widetilde{P}_{bc})\\ +(1-\widetilde{P}_{rb}(n-1))\widetilde{P}_{sc}(1-\widetilde{P}_{hc}\widetilde{P}_{cc}), & 2\le n\le N.\end{cases} \tag{23}$$

Therefore, $\widetilde{P}_s(n)$ can be calculated as follows ($2\le n\le N$):

$$\widetilde{P}_s(n)=[\widetilde{P}_{rb}(n-1)\widetilde{P}_{sc}\widetilde{P}_{bc}\widetilde{P}_{rc} + (1-\widetilde{P}_{rb}(n-1))\widetilde{P}_{sc}\widetilde{P}_{hc}\widetilde{P}_{cc}\widetilde{P}_{rc}](1-P_e). \tag{24}$$

As for ACK packets, they do not have **SC**, **RC**, and **RBC**. We set transmission delay of an ACK packet to T_t^a, then we calculate the ACK packet's STP as follows:

$$\widetilde{P}_a=(1-P_e(L_b^a))\widetilde{P}_{hc}(T_t^a)\widetilde{P}_{cc}(T_t^a). \tag{25}$$

3) Modeling of S-FAMA: In Slotted Floor Acquisition Multiple Access (S-FAMA) protocol, nodes compete for channel via RTS/CTS handshake, and only send packets at the beginning of a slot [19]. In Fig. 7, when a receiver receives only one RTS packet in a slot, it replies a CTS packet to the sender. Then the sender transmits data packets in next slots. To avoid data collisions, if a node receives unexpected control packets from neighbors, it transforms to backoff state until receives a final ACK from the receiver. In this section, we discuss all collision types based on handshake competition and deduce the STP.

In S-FAMA, nodes have five states: A) a node sends RTS packets; B) a node sends CTS packets. C) a node enters backoff state due to failure of channel competition; D) a node sends data packets; and E) a node is in the backoff state, because its neighbors are transmitting data packets. We define $\hat{T}_a, \hat{T}_b, \hat{T}_c, \hat{T}_d$, and $\hat{T}_e$ as the time of these five events, and their specific values will be presented in the next section.

Specially, we define the first four events as a whole called "data packets service". We assume that one successful handshake transmits N_d data packets, and each packet's latency

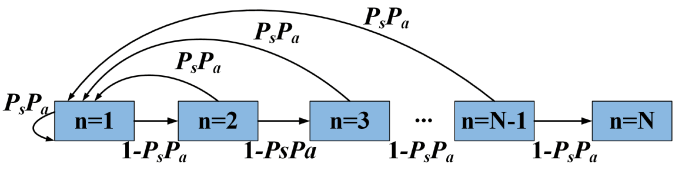

Fig. 8. Markov chain model for retransmission.

is $\hat{T}_s$. Therefore, we obtain $N_d\hat{T}_s = \hat{T}_a + \hat{T}_b + \hat{T}_c + \hat{T}_d$. Considering a long enough period $\hat{T}_l$, nodes are either in data packets service state or event E's backoff state. We denote $\hat{T}_l$ as $\hat{T}_l = N_d\hat{T}_s + \hat{T}_e$.

If a node transmits data packets successfully, the precondition is that the node obtains access to channel. We define event F as a successful handshake in one slot, and probability $\hat{P}(F|A)$ is a crucial value in this protocol. Three conditions should be satisfied: 1) no errors occur in the RTS packet; 2) no errors occur in the CTS packet; and 3) neighbors of the sender and receiver do not compete the channel in the same slot.

The probability that a node sends a RTS packet in current slot is a conditional probability $\hat{P}(A|\neg E)$. During the period $\hat{T}_l$, the probability that a node wants to send a RTS packet is defined as $\hat{\rho}_r = \min\{\lambda\hat{T}_l, 1\}$. Therefore, $\hat{P}(A|\neg E)$ can be calculated as follows:

$$\hat{P}(A|\neg E) = \frac{\hat{\rho}_r \frac{\hat{T}_a}{\hat{T}_l}}{1 - \frac{\hat{T}_e}{\hat{T}_l}}. \tag{26}$$

In addition, we define L_b^c as control packet bits. To satisfy the conditions in the last paragraph, $\hat{P}(F|A)$ can be denoted as follows:

$$\hat{P}(F|A) = (1 - P_e(L_b^c))^2(1 - \hat{P}(A|\neg E))^{\hat{n}}, \tag{27}$$

where $\hat{n}$ is the number of neighbors.

As for data packets and ACK packets, they can be transmitted successfully, as long as no packet errors occur. We set successful transmission probability of these two packets as $\hat{P}_s$, and $\hat{P}_a$, which can be denoted as: $\hat{P}_s = 1 - P_e$, and $\hat{P}_a = 1 - P_e(L_b^a)$.

B. Packet Service Time for Different MAC Protocols

In this subsection, we deduce retransmission number based on STP and Markov chain model, to design Packet Service Time (PST) models for different MAC protocols.

1) Markov Chain Model for Retransmission: As represented in Fig. 8, a complete communication means that both the data packet and the ACK packet are all transmitted successfully. P_s denotes the probability that a data packet can be transmitted successfully. P_a is the STP of an ACK packet (Here utilizes a uniform notation for all protocols). The probability that a node transmits a packet n times is defined as follows:

$$P_n = \begin{cases} (1 - P_s(n)P_a)^{n-1}P_s(n)P_a, & 1 \le n \le N-1; \\ (1 - P_s(n)P_a)^{n-1}, & n = N. \end{cases} \tag{28}$$

Based on (28), we define average transmission times of a node as follows:

$$T_n = \sum_{n=1}^{N} nP_n. \tag{29}$$

2) Modeling of TDMA: We first discuss the slot length in TDMA, which is determined by transmission delay and propagation delay. Therefore, the slot length $\dot{T}_{st}$ is designed as follows:

$$\dot{T}_{st} = 2T_{pd} + \frac{L}{TR} + \frac{L_a}{TR} + 2\frac{d_{\max}}{c}, \tag{30}$$

where T_{pd} is the preamble delay, and $d_{\max}$ is the maximum propagation distance between two nodes in the network.

When a node fails to transmit during one slot, it wastes m slots to wait the next transmission slot. We put $\dot{P}_s$ and $\dot{P}_a$ into (28), and calculate $\dot{T}_n$ via (29). Therefore, PST is calculated as follows:

$$\dot{T}_s = m\dot{T}_{st}(\dot{T}_n - 1) + \dot{T}_{st}. \tag{31}$$

Finally, we solve $\dot{T}_s$ value via (7), (8), and (31).

3) Modeling of ALOHA: In ALOHA, after sending a data packet, the node waits W_a time to receive an ACK packet. If W_a is time out, the node will back off b_o time before the retransmission. We calculate the transmission delay and the propagation delay as $T_t = \frac{L_b}{R} + T_{pd}$ and $T_{ij} = \frac{d_{ij}}{c}$, where d_{ij} denotes the distance between arbitrary node i and node j. Therefore, $W_a = T_t + T_t(L_b^a) + 2T_{ij} + T_{pg}$, where T_{pg} is the guard time of packets. We put $\widetilde{P}_s$ and $\widetilde{P}_a$ into (28), and calculate $\widetilde{T}_n$ via (29). Therefore, PST is calculated as follows:

$$\widetilde{T}_s = (W_a + b_o)(\widetilde{T}_n - 1) + (T_t + 2T_{ij} + T_t(L_b^a)). \tag{32}$$

We finally solve $\widetilde{T}_s$ value via $\widetilde{\rho}$, (24), (25), and (32) these four simultaneous equations.

4) Modeling of S-FAMA: For handshake-based protocols, both control packets and data packets are allowed to be retransmitted. Our PST model considers retransmission of RTS packets and data packets simultaneously.

The slot length $\hat{T}_{st}$ is denoted as $\hat{T}_{st} = T_t(L_b^a) + T_{ij}$. Then we put $\hat{P}_s$ and $\hat{P}_a$ into (28), and calculate $\hat{T}_n$ via (29). We define n_d as the number of slots used to transmit one data packets, which is calculated as $n_d = \lceil \frac{T_t + T_{ij}}{\hat{T}_{st}} \rceil$. S-FAMA transmits a RTS packet with n_s slots, and n_s is calculated as $n_s = \frac{1}{\hat{P}(F|A)}$.

Based on analysis of STP model, we can calculate that $\hat{T}_a = n_s\hat{T}_{st}$, $\hat{T}_b = \hat{T}_{st}$, $\hat{T}_c = 2n_s\hat{T}_{st}$, $\hat{T}_d = [(\hat{T}_n - 1)(n_d + 1)\hat{T}_{st} + (n_d + 1)\hat{T}_{st}]N_d$, and $\hat{T}_e = \hat{T}_d$. Then we calculate PST as follows:

$$\hat{T}_s = \frac{\hat{T}_a + \hat{T}_b + \hat{T}_c + \hat{T}_d}{N_d}. \tag{33}$$

By combining (33) with $\hat{T}_e$, $\hat{P}(F|A)$, $\hat{P}_s$, and $\hat{P}_a$, $\hat{T}_s$ is solved.

C. Network Performance Metrics

We calculate nodal throughput, delay, and energy consumption based on STP model and PST model. (This section utilizes a uniform notation for all protocols.)

Nodal Throughput: On average, each node transmits L_b bits every T_n times with T_s latency. Therefore, the nodal throughput is calculated as follows:

$$T_h = \rho \frac{L_b[1-(1-P_s)^{T_n}]}{T_s}. \tag{34}$$

Delay: A packet delay includes transmission, propagation, and queuing delay. Based on PST model, final delay is calculated via Pollaczek-Khinchin formula [20] as follows:

$$S_t = T_s + \frac{\lambda {T_s}^2}{2(1-\rho)}. \tag{35}$$

Specifically, $1-\rho < 0$ or the network is congested.

Energy consumption: Energy consumption relies on transmission power and transmission delay. We first define T_{dt} as the transmission delay for one complete communication, which is calculated as follows:

$$T_{dt} = 2T_{pd} + \frac{L_b}{R} + \frac{L_b^a}{R}. \tag{36}$$

Transmission power P_{sp} is set on the basis of propagation distance and channel quality. Considering retransmission, the energy consumption of TDMA protocol and ALOHA protocol is calculated as follows:

$$E = P_{sp} T_n T_{dt}. \tag{37}$$

As for S-FAMA, control packets also consume energy. We have analyzed that n_s RTS packets and one CTS packet are transmitted before the data transmission. Therefore, the energy consumption of S-FAMA is denoted as follows:

$$E = P_{sp} \frac{L_b^c}{R}(n_s+1) + P_{sp} T_n T_{dt}. \tag{38}$$

V. Simulation Experiments

A. Simulation Settings

We evaluate nodal throughput, packet average delay, and energy consumption with different MAC protocols under various network scenarios. In the following experiments, all models' results are calculated by MATLAB. We set node center frequency f to 24 kHz, the bandwidth is 6 kHz, data packet size L to 1600 bits, ACK size L_a to 120 bits, preamble T_{pd} to 0.5 s, and maximum transmission times N to 4. BPSK, QPSK, 8QAM, 16QAM, and 64QAM five transmission modes in [21], [22] are adopted in this paper to provide various packet errors and transmission rates. We sort these five modes in ascending order of transmission rate (BPSK as mode1, QPSK as mode2, 8QAM as mode3, 16QAM as mode4, and 64QAM as mode5). Under the same environment, the mode with a larger transmission rate results in higher packet error. In particular, we just discuss general parameters, and other parameter settings will be defined in subsequent specific experiments.

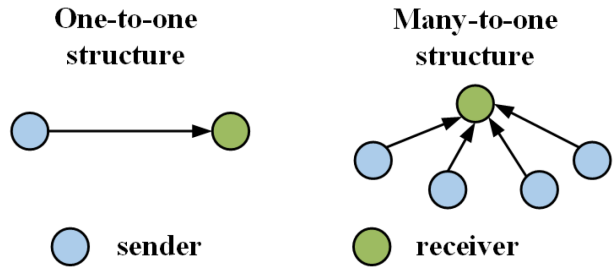

Fig. 9. Two basic structural relationships between nodes from the perspective of a single receiver.

TABLE I
Differences Between MPAF and Other Underwater MAC Performance Analysis Models

Models	Half-duplex Communication	Random Backoff	Long Propagation Delay	Retransmission
MPAF	✓	✓	✓	✓
PDPE	×	×	✓	✓
BTP	✓	×	×	×
TPM	×	×	✓	×
PA	×	×	×	×

From the perspective of a single receiver, senders and receivers have two basic structural relationships as represented in Fig. 9. In the first structure, each sender has its own receiver, called one-to-one (O2O). In the second structure, many senders have the same receiver, called many-to-one (M2O). These two structures are the basis of any UAN. Therefore, we analyze MAC protocols' performance based on these two basic structures.

B. Analysis of MPAF Authenticity

In this set of simulations, we compare nodal throughput results of MPAF and models in [5], [6], [7], [8] to answer the following question:

- *RQ1:* Can the proposed MPAF provide more accurate analysis results than existing models?

Baseline methods: We define models in [5], [6], [7], [8] as Toward Practical Mac model (TPM), Packet Delay and Packet Error model (PDPE), Busy Terminal Problem model (BTP), and Persistent ALOHA model (PA), respectively. The differences between these models are shown in Table I.

- TPM proposed STP and PST models for S-FAMA protocol. However, it simplifies the backoff scheme of S-FAMA and ignores packet error rate and retransmission in actual UANs.
- PDPE also proposed an S-FAMA model. Compared with TPM, it analyzes different conditions of channel competition failure and considers packet error rate and retransmission. However, it still simplifies S-FAMA's backoff scheme.
- BTP proposed an ALOHA model for UANs, which considers half-duplex communication to analyze different data loss types. However, it ignores random backoff and retransmission, failing to evaluate **RBC** collision. Moreover, it neglects the impacts of long propagation delay on packet

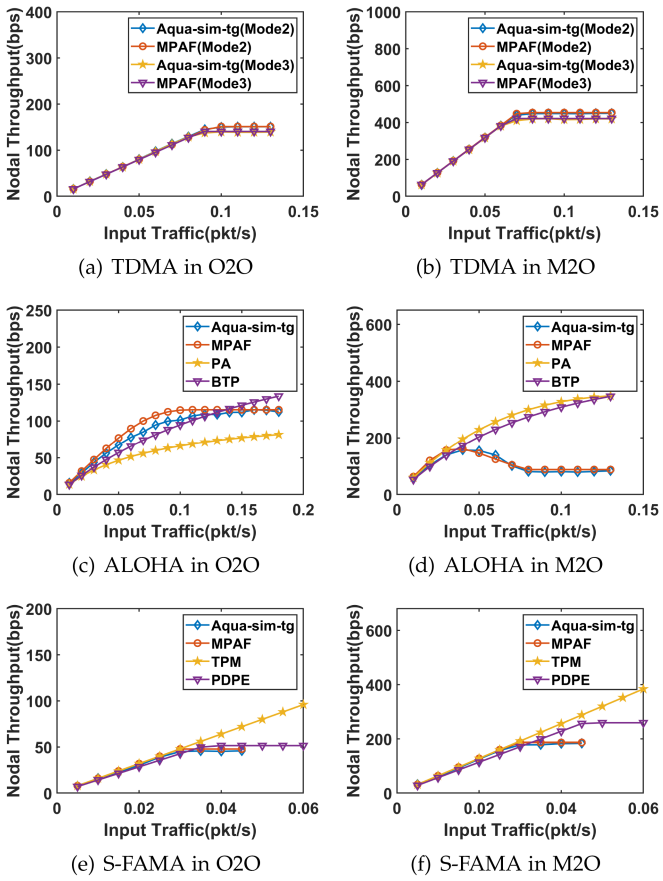

Fig. 10. Comparison results about model authenticity.

queue and long-term communications and exactly follows the Poisson distribution to build the model, which does not conform to real UAN scenarios.

- PA proposed an ALOHA model for UANs but analyzed underwater communications entirely based on terrestrial networks.

Moreover, results of Aqua-Sim-tg are used to evaluate models' authenticity. Aqua-Sim-tg is the third-generation simulator of UAN based on NS-3, and real sea trials' data have validated its authenticity in [23]. The simulator supports simulating underwater channel with actual marine environmental data.

Specific settings: Considering the sparsity of actual UAN, we set a basic network structure with five nodes. For the O2O chain structure, distance between two adjacent nodes is set to 2 km. For the M2O structure, it has four senders and one receiver, and the distance between sender and receiver is 2 km. The average Signal to Noise Ratio (SNR) is set to 8 dB, and we evaluate nodal throughput by varying input traffic from 0.01 packet/s (pkt/s) to 0.2 pkt/s.

Results analysis (RQ1): We observe nodal throughput variation before the network congestion in Fig. 10. Fig. 10(a) and (b) show the results of TDMA protocol. We did not find other TDMA models for UAN, thus, we compare two modes (mode2 and mode3 mentioned in Section V-A) in this experiment. Due to the simple design of TDMA protocol, MPAF analyzes accurate performance by integrating retransmission. As for ALOHA protocol, we can observe that MPAF is more realistic than other two models. This is because other models ignore unique UAN characteristics and fail to analyze all data loss types. Especially in Fig. 10(d), PA and BTP can not reflect severe re-collisions caused by random backoff. In addition, Fig. 10(e) and (f) indicate that MPAF evaluates authentic S-FAMA performance. This is because MPAF analyzes events of handshake competition based on UAN characteristics, and considers retransmission of control packets and data packets at the same time. After verifying the authenticity of MPAF, we can use it to analyze performance from multi-aspects in theory.

C. Performance Under Different Channel Conditions

In this set of simulations, we compare the performance of different MAC protocols via MPAF under different channel conditions to answer the following questions:

- *RQ2:* For all basic MAC protocols, what is the lower bound of channel quality for each transmission mode to work optimally?
- *RQ3:* Which MAC protocol can be adapted to UANs with low channel quality?

Specific settings: In this set of experiments, we set input traffic λ to 0.02 pkt/s. The distance between two adjacent nodes is 2 km, and the transmission power is 3 w. Then we vary SNR range from 4 dB to 15 dB, covering different channel qualities based on some public sea trial results and our own sea trial experience [24], [25], [26].

Modes Comparison (RQ2): In Tables II and III, we observe that mode1 performs better than other modes under low-SNR conditions. This is because mode1 has lower packet error than other modes, due to the smaller code rate. Although other modes provide higher transmission rate, retransmissions caused by packet error aggravate delay under low-SNR conditions. By comparison, mode1's transmission delay is acceptable, because mode1 provides more stable transmissions. If the channel provides moderate SNR, mode2 is a better choice than mode1, because mode2 provides a higher transmission rate. When both these two modes work normally, mode2 performs low transmission delay and energy consumption. Unlike the first three modes, mode4 and mode5 fail to transmit stably even under a high-SNR (15 dB) condition. They are hardly used in UANs, due to harsh marine environments.

Protocols Comparison (RQ3): In Table II, nodal throughput of ALOHA is very close to results of TDMA and S-FAMA, which demonstrates ALOHA has low collisions when input traffic is small (0.02 pkt/s in this set of experiments). In such a condition, it performs the lowest delay due to the simplest transmission scheme. However, nodal throughput of ALOHA is smaller than other protocols in Table III. This is because M2O structure has more senders, and collisions are more severe at the receiver. TDMA and S-FAMA avoid data collisions by dividing transmission time and reserving the channel. Therefore, they perform better nodal throughput when the network is not congested. These two protocols have longer delay than ALOHA, due to collision avoidance schemes. The phenomenon is greatly obvious in M2O structure, because TDMA and S-FAMA require

TABLE II
OPTIMAL PERFORMANCE OF EACH MODE FOR DIFFERENT MAC PROTOCOLS IN THE O2O STRUCTURE

	SNR[1](dB)			Nodal Throughput (bps)			Delay (s)			Energy Consumption (J)		
	TDMA	ALOHA	S-FAMA	TDMA	ALOHA	S-FAMA	TDMA	ALOHA	S-FAMA	TDMA	ALOHA	S-FAMA
Mode1	6	7	6	32.00	31.64	32.00	16.79	6.98	56.14	12.06	15.31	13.70
Mode2	9	9	9	32.00	31.91	32.00	14.63	5.34	56.09	8.03	9.32	9.67
Mode3	13	11	13	32.00	31.93	32.00	13.96	5.02	56.30	6.70	7.70	8.35
Mode4	15	15	15	31.99	31.90	31.99	14.26	5.00	55.94	6.27	7.02	7.93
Mode5	15	15	15	7.77	5.97	4.43	58.47	14.71	60.95	14.64	14.97	23.84

[1] Displayed SNR values are lower bounds for each mode to work at its best in the current condition.

TABLE III
OPTIMAL PERFORMANCE OF EACH MODE FOR DIFFERENT MAC PROTOCOLS IN THE M2O STRUCTURE

	SNR[1](dB)			Nodal Throughput (bps)			Delay (s)			Energy Consumption (J)		
	TDMA	ALOHA	S-FAMA	TDMA	ALOHA	S-FAMA	TDMA	ALOHA	S-FAMA	TDMA	ALOHA	S-FAMA
Mode1	6	9	6	128.00	101.47	128.00	24.34	11.63	38.21	12.06	21.89	13.62
Mode2	9	10	8	128.00	123.53	128.00	20.91	6.75	38.43	8.03	11.07	9.63
Mode3	13	14	13	128.00	125.93	128.00	19.87	5.82	38.27	6.70	8.62	8.26
Mode4	15	15	15	127.99	124.78	127.99	20.33	5.80	38.11	6.27	7.88	7.83
Mode5	15	15	15	31.09	16.44	21.14	153.28	15.04	40.58	14.64	15.22	23.84

[1] Displayed SNR values are lower bounds for each mode to work at its best in the current condition.

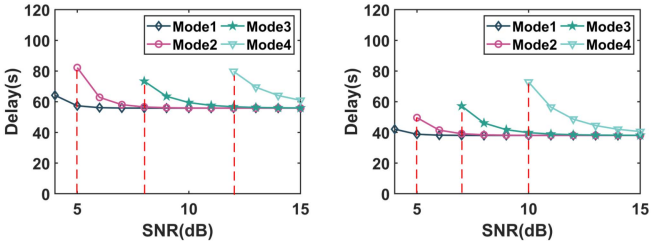

(a) Delay in O2O (b) Delay in M2O

Fig. 11. Impacts of SNR on delay of S-FAMA protocol with different structures.

waiting more slots to transmit data and reserve the channel, respectively. Especially for S-FAMA, in Fig. 11, we can observe that some delay results are missing when SNR is small, which means the network is congested. This is because control packets without restriction increase network collisions, then aggravate data packets' waiting time. Network with S-FAMA protocol is more prone to congestion. According to (35), $\rho < 1$ or else the network is congested, and delay for one packet can not be calculated theoretically. If the collision is within a tolerable range, the random access-based protocol provides less delay under low-SNR conditions. Otherwise, we sacrifice some latency and employ TDMA protocol.

D. Performance Under Different Input Traffics

In this set of simulations, we set SNR to a moderate value of 9 dB based on the conclusion of Section V-C. In this way, we try to avoid impacts of channel quality to answer the following question:

- *RQ4:* Under good underwater communication environments, what is the maximum network capacity of different protocols? Which protocol is optimal for the UAN with large traffic?

Specific settings: In this set of experiments, the distance between two adjacent nodes is 2 km, and the transmission power is 3 w. We set SNR to 9 dB and transmission mode to mode2. Then we change input traffic λ from 0.01 pkt/s to 0.12 pkt/s.

Protocols Comparison (RQ4): Throughput in Fig. 12(d) is larger than in Fig. 12(a). This is because the receiver receives more packets from multiple senders in M2O structure. TDMA provides the maximum capacity for UANs in both two structures. This is because TDMA has no collisions, due to the noncompetitive transmission scheme. In Fig. 12(a), S-FAMA performs the worst throughput. We analyze reasons as follows: when λ is small, handshake fails to play advantages, due to limited data packets; when λ becomes larger, control packets conflict seriously and reduce network performance. As for ALOHA, we can observe that throughput decreases dramatically before the network gets congested. This is because that random backoff makes conflicting packets collide again. This phenomenon in Fig. 12(d) (the throughput reduction is 108 bps) is more conspicuous and appears much earlier than in Fig. 12(a) (the throughput reduction is 14 bps), because there is only one receiver for multiple senders in M2O structure, collision probability is greater. Impacts of such re-collisions are more serious than control packets' collisions in S-FAMA, thus ALOHA performs the lowest throughput in M2O structure.

Comparing Fig. 12(b) and (e), we can observe that delay becomes longer as the increase of λ for TDMA, and the UAN in M2O structure congests more quickly. This is because multiple senders mean more slots in M2O structure, which results in longer queuing delay. As λ increases, more slots make UAN congest more quickly. For S-FAMA, we can observe that delay of O2O structure is higher than M2O structure. This is because delay of backoff state is longer in O2O structure. In O2O structure, each node has its own receiver. A node backs off more frequently to avoid influencing neighbors' transmission. However, some backoffs are invalid and do not affect the actual transmission, but introduce more waiting delay. Based on the analysis in Tables II and III, we observe that the congestion of ALOHA protocol occurs later than TDMA and S-FAMA in Fig. 12. This is because nodes in ALOHA protocol do not need

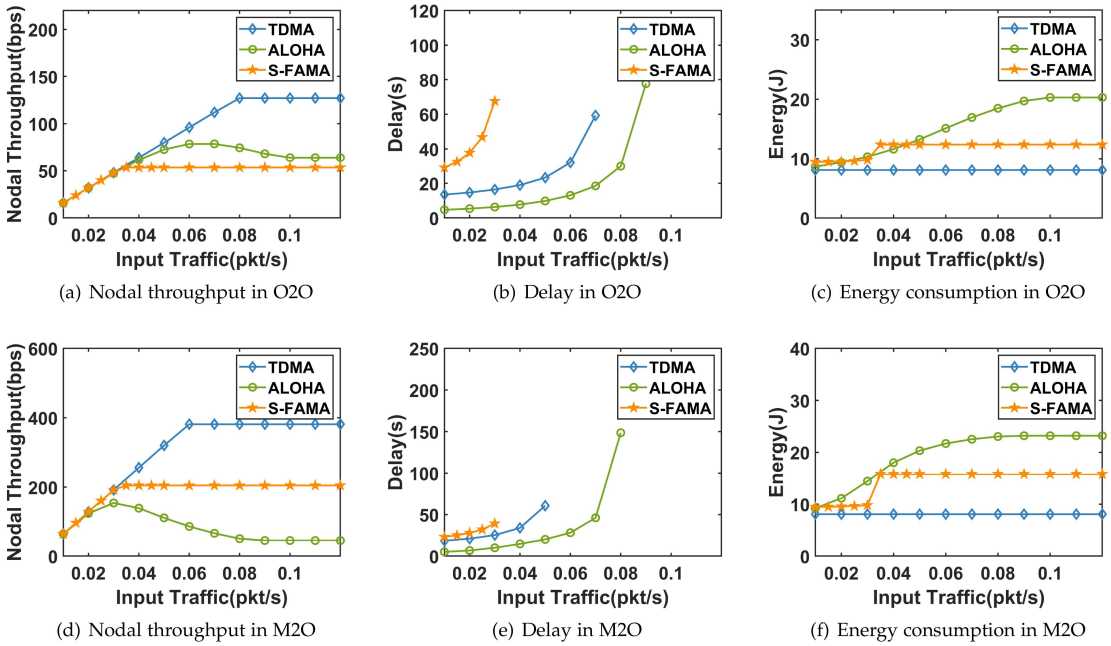

(a) Nodal throughput in O2O (b) Delay in O2O (c) Energy consumption in O2O

(d) Nodal throughput in M2O (e) Delay in M2O (f) Energy consumption in M2O

Fig. 12. Impacts of input traffic on nodal throughput, delay, and energy consumption of three protocols with different structures.

to wait for their own slots or reserve the channel. Therefore, the waiting delay is reduced. However, random transmissions result in high collisions. Although the network with ALOHA protocol congests more slowly, capacity is not satisfactory, as represented in Fig. 12(a) and (d). On the other hand, delay results in Fig. 12(b) and (e) are proved again that the reduction in Fig. 12(a) and (d) is caused by re-collisions rather than network congestion.

For TDMA, energy consumption is the same in two structures in Fig. 12(c) and (f). This is because the number of transmission times is only relevant to packet error rate in TDMA protocol. Therefore, energy consumption of one packet is constant without changing transmission power and transmission mode. For ALOHA, nodes consume more energy as λ becomes larger. The reason is that more collisions lead to more retransmissions. When the network is congested, the transmission number becomes constant, and energy consumption no longer increases. For S-FAMA, energy consumption increases slowly before network congestion, as represented in Fig. 12(c) and (f). This is because the increased part is only related to control packets, and handshake can easily succeed when λ is small. When the network is congested, the handshake number increases quickly during a short period with an increase of λ. Therefore, energy consumption first becomes larger, then tends to be stable.

Based on the above analysis via MPAF, S-FAMA and ALOHA have serious collisions in UANs when the input traffic is great. TDMA performs stable in both nodal throughput and energy consumption, which is an appropriate selection providing high capacity with low costs for high-traffic UANs.

E. Performance Under Different Network Densities

In actual UANs, nodes are close to each other in dense networks and far apart in sparse networks. In this set of simulations, we compare the performance of different MAC protocols via MPAF under different propagation distances to answer the following questions:

- *RQ5:* What are effects of network densities on MAC protocols? Which protocol is suitable for dense UANs, and which is suitable for sparse UANs?

Specific settings: In this set of experiments, we set input traffic λ to 0.02 pkt/s, and SNR to 9 dB. Then we change the distance between two adjacent nodes from 1 km to 5 km. and correspondingly increases transmission power from 3 w to 80 w.

Protocols Comparison (RQ5): In this set of experiments, we set a small input traffic 0.02 pkt/s. Under such a condition, we observe TDMA and ALOHA provide stable nodal throughput in Fig. 13(a) and (d). For TDMA, data loss is only related to packet error. Changing propagation distance does not influence packet transmission time and the retransmission number. On the other hand, the current small input traffic does not cause network congestion. Therefore, nodal throughput in TDMA is a constant. For ALOHA, mode2 provides a high transmission rate in the current condition, and there are fewer collisions in Fig. 13(a). However, the throughput of ALOHA is smaller than TDMA in Fig. 13(d), which means ALOHA is not stable in M2O structure. This phenomenon demonstrates again that re-collisions are an essential issue in random access-based protocols. As for S-FAMA, throughput decreases as increase of propagation distance. This is because the network is congested caused by a long reservation period. Due to the complex handshake mechanism, S-FAMA needs more time to transmit data packets, and is more sensitive to propagation distance than the other two protocols.

In Fig. 13(b) and (e), we can observe that the delay becomes larger with the increase of propagation distance for TDMA and ALOHA. This is because longer distance means longer propagation delay. Especially for TDMA, when there are more slots in M2O structure as represented in Fig. 13(e), an increase in the single slot length causes a multiplicative increase in the

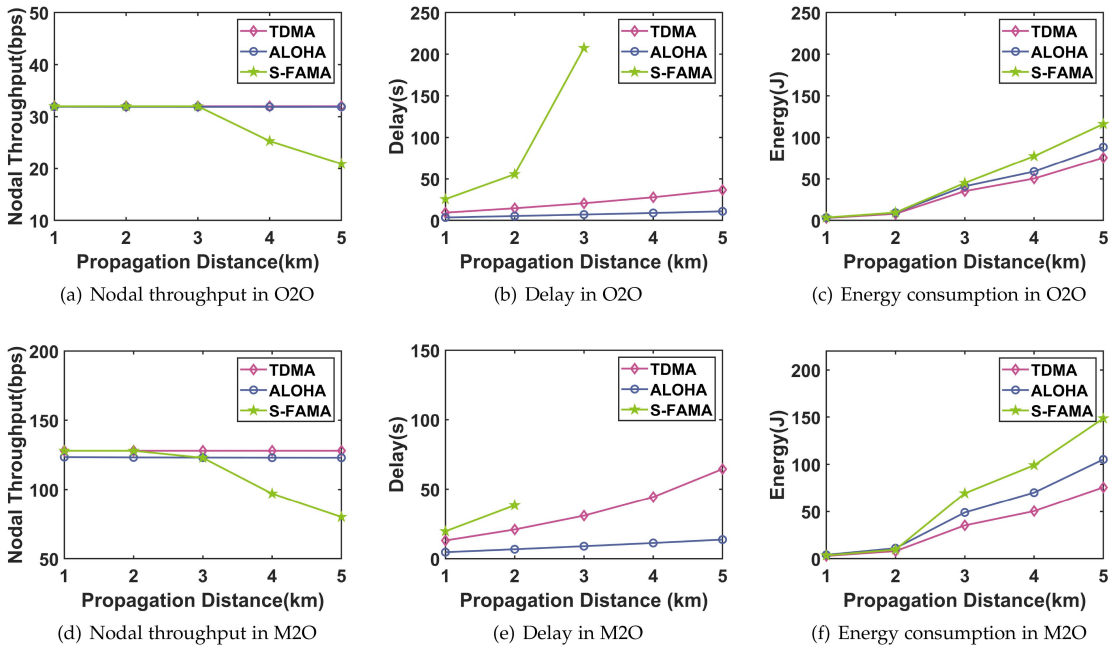

(a) Nodal throughput in O2O (b) Delay in O2O (c) Energy consumption in O2O

(d) Nodal throughput in M2O (e) Delay in M2O (f) Energy consumption in M2O

Fig. 13. Impacts of propagation distance on nodal throughput, delay, and energy consumption of three protocols with different structures.

total delay. In addition, delay results further verify that the network adopting S-FAMA protocol is more prone to congestion when propagation distance increases. On the one hand, lager propagation distance means longer slot length, and nodes waste more time during backoff. On the other hand, the time used to reserve a channel also increases due to longer propagation delay.

In Fig. 13(c) and (f), we can observe that nodes consume more energy as propagation distance increases. This is because transmission power is improved to deal with greater attenuation caused by longer propagation distance. ALOHA consumes more energy in M2O structure than O2O structure, which echoes the conclusion of Fig. 13(d) and (a): the nodal throughput reduction is caused by re-collisions. Therefore, ALOHA has more retransmissions in M2O structure. S-FAMA consumes the most energy. This is because control packets face serious collisions, and the constant handshaking results in high energy consumption.

The propagation distance influences the successful handshaking probability of S-FAMA. Moreover, long propagation delay aggravates slot length in TDMA. When the input traffic is small, long distance even decreases collisions of low transmission rate mode in ALOHA. If the data loss is tolerated, ALOHA provides the lowest delay in long-distance UANs. When the distance is small, TDMA can provide the most robust communication.

F. Discussion

We summarize the above simulation results, select appropriate MAC protocols for various scenarios, and provide design suggestions for underwater MAC protocols.

Transmission modes: Due to harsh underwater acoustic environments, high transmission rate modes like mode 4 and mode 5 are almost unusable in underwater MAC protocols. Mode1 provides the most reliable transmission. If the channel quality is favorable, we can consider mode2 and mode3 to improve the transmission rate. MPAF also supports evaluating MAC protocols with other transmission modes, as long as there is a correspondence between packet error rate and SNR.

Application scenarios: For time-sensitive UANs, random access-based protocols perform the lowest delay. However, the precondition is to observe via MPAF whether the data is within an acceptable range. For reliability-sensitive UANs, TDMA-based protocols provide the most robust transmission, since the data loss is only related to the channel quality.

Protocol design suggestions: Based on the above experiments, we find that slot length and the number of waiting slots strongly impact TDMA-based protocols' performance. If we select TDMA as a basic protocol for a specific UAN, the focus of the improvement is increasing the concurrency of the same slot. For random access-based protocols, decreasing collisions is a consensus solution to improve performance. In this paper, we find a new type of collision **RBC** caused by retransmissions, and such collision seriously affects the performance in M2O structure. Therefore, when we modify random access-based protocols, **RBC** should be addressed. For handshake-based protocols, although the reservation scheme decreases collisions of data packets, extra control packets introduce new collisions. A promising design is to decrease control packets' collisions. Therefore, it can ensure data transmission without collisions, as well as avoid long waiting delay caused by time division.

The practicality of MPAF: The above experiments prove that MPAF can output theory performance boundary with given parameters, or parameter values that satisfy certain performance constraints. MPAF is applicable in both 2D and 3D underwater environments since its significant factors are parameterized, and these parameters can be obtained in different dimensions. Although MPAF analyzes three basic MAC protocols, these

protocols almost cover major MAC problems. In general, newly designed protocols solve more problems than basic protocols, which means the analysis of new protocols is simpler than basic protocols. For example, S-ALOHA [27] is an improved ALOHA protocol, requiring each sender to transmit at the beginning of a slot. In this way, collisions **SC** and **CNC** do not exist in S-ALOHA. Therefore, we can simplify the ALOHA model to evaluate S-ALOHA's performance.

VI. Conclusion and Future Work

In this paper, a MAC protocols' performance analysis framework, called MPAF, is proposed for UANs. MPAF includes two models, STP model and PST model, to select the optimal MAC protocol for various scenarios by analyzing nodal throughput, delay, and energy consumption. In STP model, data loss types are analyzed by considering unique UANs' characteristics to obtain more accurate STP results of different MAC protocols. Then, we utilize Markov chain to deduce the number of retransmissions and further build a PST model based on queuing theory. Plentiful simulation results show: 1) MPAF can evaluate MAC protocols' performance accurately. 2) MPAF can find the best basic protocol from multiple candidates. 3) MPAF can provide optimal network and communication parameters for a specific MAC protocol. 4) MPAF can show the problem of each type of protocol, providing directions for improvements.

Future Work: In this paper, we analyze the simple one-hop performance of different MAC protocols. For multi-hop network performance, the analysis model should consider the effects of routing protocols. Moreover, nodes are not equal in multi-hop networks, which is a challenging problem of analyzing performance. In future work, we will combine routing and MAC protocols to evaluate multi-hop network performance. Moreover, we will design real sea trials, collect various time-varying environmental information, and further verify MPAF with real experimental data.

References

[1] G. Han, X. Long, C. Zhu, M. Guizani, and W. Zhang, "A high-availability data collection scheme based on multi-AUVs for underwater sensor networks," *IEEE Trans. Mobile Comput.*, vol. 19, no. 5, pp. 1010–1022, May 2020.

[2] S. Song, J. Liu, J. Guo, C. Zhang, T. Yang, and J. Cui, "Efficient velocity estimation and location prediction in underwater acoustic sensor networks," *IEEE Internet Things J.*, vol. 9, no. 4, pp. 2984–2998, Feb. 2022.

[3] S. Song, J. Liu, J. Guo, J. Wang, Y. Xie, and J.-H. Cui, "Neural-network-based AUV navigation for fast-changing environments," *IEEE Internet Things J.*, vol. 7, no. 10, pp. 9773–9783, Oct. 2020.

[4] P. Mandal, S. De, and S. S. Chakraborty, "Characterization of aloha in underwater wireless networks," in *Proc. Nat. Conf. Commun.*, 2010, pp. 1–5.

[5] Y. Zhu, Z. Peng, J.-H. Cui, and H. Chen, "Toward practical MAC design for underwater acoustic networks," *IEEE Trans. Mobile Comput.*, vol. 14, no. 4, pp. 872–886, Apr. 2015.

[6] Y. Song and P.-Y. Kong, "Optimizing design and performance of underwater acoustic sensor networks with 3D topology," *IEEE Trans. Mobile Comput.*, vol. 19, no. 7, pp. 1689–1701, Jul. 2020.

[7] Y. Zhu, Z. Zhou, Z. Peng, and J.-H. Cui, ""Busy terminal problem" and implications in underwater acoustic networks," in *Proc. 7th Int. Conf. Underwater Netw. Syst.*, 2012, pp. 1–2.

[8] Y. Zhang, "Performance of P-persistent slotted aloha for underwater sensor networks," in *Proc. Int. Conf. Comput. Netw. Commun.*, 2014, pp. 583–587.

[9] K. Chen, M. Ma, E. Cheng, F. Yuan, and W. Su, "A survey on MAC protocols for underwater wireless sensor networks," *IEEE Commun. Surveys Tut.*, vol. 16, no. 3, pp. 1433–1447, Third Quarter 2014.

[10] S. N. Le, Y. Zhu, Z. Peng, J.-H. Cui, and Z. Jiang, "PMAC: A real-world case study of underwater MAC," in *Proc. 8th Int. Conf. Underwater Netw. Syst.*, 2013, pp. 1–8.

[11] R. Zhang, X. Cheng, X. Cheng, and L. Yang, "Interference-free graph based TDMA protocol for underwater acoustic sensor networks," *IEEE Trans. Veh. Technol.*, vol. 67, no. 5, pp. 4008–4019, May 2018.

[12] E. P. C. Júnior, L. F. Vieira, and M. A. Vieira, "UW-SEEDEX: A pseudorandom-based mac protocol for underwater acoustic networks," *IEEE Trans. Mobile Comput.*, vol. 21, no. 9, pp. 3402–3413, Sep. 2022.

[13] S. Jiang, "State-of-the-art medium access control (MAC) protocols for underwater acoustic networks: A survey based on a MAC reference model," *IEEE Commun. Surv. Tut.*, vol. 20, no. 1, pp. 96–131, First Quarter 2018.

[14] L. Bai, R. Han, J. Liu, J. Choi, and W. Zhang, "Random access and detection performance of Internet of Things for smart ocean," *IEEE Internet Things J.*, vol. 7, no. 10, pp. 9858–9869, Oct. 2020.

[15] P. Xie and J.-H. Cui, "Exploring random access and handshaking techniques in large-scale underwater wireless acoustic sensor networks," in *Proc. OCEANS*, 2006, pp. 1–6.

[16] C. Petrioli, R. Petroccia, and M. Stojanovic, "A comparative performance evaluation of MAC protocols for underwater sensor networks," in *Proc. OCEANS*, 2008, pp. 1–10.

[17] R. Jain, *The Art of Computer Systems Performance Analysis: Techniques for Experimental Design, Measurement, Simulation, and Modeling*. Hoboken, NJ, USA: Wiley, 1991.

[18] L. Pu et al., "Comparing underwater MAC protocols in real SEA experiments," *Comput. Commun.*, vol. 56, pp. 47–59, 2015.

[19] M. Molins and M. Stojanovic, "Slotted Fama: A Mac Protocol for Underwater Acoustic Networks," in OCEANS 2006-Asia Pacific, 2006, pp. 1–7.

[20] M. Guizani, A. Rayes, B. Khan, and A. Al-Fuqaha, *Network Modeling and Simulation: A Practical Perspective*. Hoboken, NJ, USA: Wiley, 2010.

[21] Z. Zhou, S. Le, and J.-H. Cui, "An OFDM based MAC protocol for underwater acoustic networks," in *Proc. 5th Int. Workshop Underwater Netw.*, 2010, pp. 1–8.

[22] H. Yan et al., "DSP based receiver implementation for OFDM acoustic modems," *Phys. Commun.*, vol. 5, no. 1, pp. 22–32, 2012.

[23] J. Guo, J. Liu, S. Song, C. Zhang, H. Chen, and J.-H. Cui, "Aqua-Psim: A semi-physical simulation platform based on NS3 for underwater acoustic network," in *Proc. 15th Int. Conf. Underwater Netw. Syst.*, 2021, pp. 1–5.

[24] P. Casari et al., "ASUNA: A topology data set for underwater network emulation," *IEEE J. Ocean. Eng.*, vol. 46, no. 1, pp. 307–318, Jan. 2021.

[25] G. Wang, M. Liu, X. Pan, Y. Gou, T. Yang, and J.-H. Cui, "Field experiment and analysis of underwater string networks based on PMAC," in *Proc. 15th Int. Conf. Underwater Netw. Syst.*, 2021, pp. 1–8.

[26] J. Zhu, X. Pan, Z. Peng, M. Liu, J. Guo, and J.-H. Cui, "uw-WiFi: Small-scale data collection network-based underwater Internet of Things," *J. Mar. Sci. Eng.*, vol. 12, no. 3, 2024, Art. no. 481.

[27] L. G. Roberts, "Aloha packet system with and without slots and capture," *ACM SIGCOMM Comput. Commun. Rev.*, vol. 5, no. 2, pp. 28–42, 1975.

Jiani Guo received the BS degree in computer science and technology from Beijing Jiaotong University, Beijing, China, in 2016. She is currently working toward the PhD degree with the College of Computer science and technology, Jilin University, Changchun, China. Her current research interests include MAC protocols design and performance analysis for underwater acoustic networks.

Shanshan Song (Member, IEEE) received the BS and MS degrees in computer science and technology from Jilin University, China, in 2011 and 2014, respectively, and the PhD degree in management science and engineering from Jilin University, China, in 2018. She is currently an associate professor with the Department of Computer science and technology, Jilin University. Her major research focuses on underwater data collection, localization and navigation and machine learning. She serves as the WUWNet' 2021 EDAS chair.

Jun Liu (Member, IEEE) received the PhD degree in computer science and engineering from the University of Connecticut, USA, in 2013. Currently, he is a professor of the School of Electronic and Information Engineering, Beihang University, Beijing, China. His major research focuses on underwater acoustic networking, time synchronization, localization, network deployment, and also interested in operating system, cross layer design. He is a member of the IEEE Computer Society.

Hao Chen received the BS degree in computer science and technology from Jilin University, Changchun, China, in 2022. He is currently working toward the PhD degree with the College of Computer science and technology, Jilin University, Changchun, China. His major research focuses on performance analysis for underwater acoustic networks.

Yuanbo Xu received the BE, ME, and PhD degrees in computer science and technology from Jilin University, Changchun, China, in 2012, 2015, and 2019, respectively. He is currently an associate professor with the Department of computer science and technology, Jilin University, Changchun. His research interests include applications of data mining, recommender system, and mobile computing. He has published some research results on journals such as the *IEEE Transactions on Multimedia*, *IEEE Transactions on Neural Networks and Learning Systems*, and conference as ICDM.

Jun-Hong Cui (Member, IEEE) received the PhD degree in computer science from the University of California, Los Angeles, in 2003. Currently, she is the professor of the College of Computer Science and Technology, Jilin University, Changchun, China. Her research interests include the design, modeling, and performance evaluation of networks and distributed systems. She is actively involved in the community as an organizer, a TPC member, and a reviewer for many conferences and journals. She is a guest editor for ACM Mobile Computing and Communications Review and Elsevier Ad Hoc Networks. She cofounded the first ACM International Workshop on UnderWater Networks (WUWNet 2006) and now serves as the WUWNet steering committee chair. She is a member of the ACM, ACM SIGCOMM, ACM SIGMOBILE, IEEE Computer Society, and IEEE Communications Society.